RSC Advances

PAPER

Cite this: *RSC Adv.*, 2022, **12**, 9473

An anthracenecarboximide-guanidine fluorescent probe for selective detection of glyoxals under weak acidic conditions†

Junwei Chen,‡[a] Yuna Lin,‡[a] Wanjin Xing,[a] Xingchen Zhang,[a] Huan Xu,*[a] Wei Wang *[b] and Kaiyan Lou *[a]

Received 3rd February 2022
Accepted 19th March 2022

DOI: 10.1039/d2ra00741j

rsc.li/rsc-advances

An anthracenecarboximide-guanidine based turn-on fluorescent probe **ANC-DCP-1** for selective detection of glyoxals (methylglyoxal and glyoxal, GOS) over formaldehyde under weak acidic conditions around pH 6.0 was reported. The probe showed great potential in studying relative GOS levels in weak acidic biological fluids such as in urine for diabetic diagnosis and prognosis, and also found application in the food industry such as for fast unique manuka factor (UMF) scale determination of Manuka honey.

Introduction

Glyoxals (GOS) including methylglyoxal (MGO) and glyoxal (GO) are structurally very similar dicarbonyl species in biological systems.[1–3] They are highly reactive glycating agents and react with proteins, DNAs, and lipids to form advanced glycation and lipoxidation end products (AGEs and ALEs), resulting in protein dysfunctions, dicarbonyl stress, and cell death.[4,5] MGO is produced mainly from glycolysis (non-enzymatic degradation of triosephosphates),[6] L-threonine metabolism,[7] and lipid peroxidation,[8] while GO is mostly generated from lipid peroxidation and autooxidation of glucose.[9,10] Aside from their similar reactivity and both being metabolites from glucose metabolism and lipid peroxidation, GOS also share their major removal pathway *via* the glyoxalase system,[3,11] and their levels are often correlated in biological systems. Upregulated GOS levels are involved in many disease states such as diabetes,[12–14] obesity,[15] cancer,[16] and Alzheimer's disease.[17] Besides, GOS also widely exist in food including cookies, yogurt, bread, and Manuka honey.[18,19] Therefore, methods for measuring GOS levels are highly desirable in GOS associated disease and dietary studies.

Traditional methods for GOS detection often requires tedious sample derivatization with *o*-phenylenediamine (OPD)-based reagents and further separation GOS adducts by HPLC or GC, which are not capable of *in situ* studies.[20] Recently, fluorescent probe based imaging methods, which utilize OPD,[21–24] 2-amino-2-phenylacetamide,[25] or 1,8-diaminonapthalene[26] as the GOS reactive group (Fig. 1a), have attracted research interests for their easy operation and *in situ* detection potentials.[27] However, most of these probes react irreversibly with GOS and also react with formaldehyde (FA), a key intermediate in one-carbon metabolism with a reactive aldehyde group.[28] Inspired by arginine-specific glycation reaction by GOS in biological systems, we recently reported **NAP-DCP** series of probes as the first reversible GOS fluorescent probes, which adopt a guanidino group as the GOS reactive group (Fig. 1b).[29] The **NAP-DCP** series of probes have pK_a values around 8.5 and mainly exist in the guanidinium form at pH 7.4. When react with GOS to form 5-membered exocyclic dihydroxyimidazolidines in equilibrium (Fig. 1b), the formed adducts have increased acidity and significant portion of deprotonation with newly emerged red-shifted absorption peak at pH 7.4, which can be selectively excited to generate the fluorescence turn-on response. The formation of 5-membered ring over 4-membered ring ensures their high selectivity for GOS over FA.[29] However, the **NAP-DCP** series of probes cannot detect GOS in acidic environment such as in human urine, which normally has pH ranging from 5.6 to 6.8.[30] In this work, we would like to explore the effect of replacement of the naphthalene group in **NAP-DCP** series of probes with an anthracene group and designed a new probe **ANC-DCP-1** adopting 1,9-anthrenecarboximide as the fluorophore (Fig. 1c). It was expected that **ANC-DCP-1** has similar reactivity and selectivity with GOS by adopting the same reactive group. Moreover, the extended conjugation system not only would afford fluorescence emission with longer wavelength, but also would help to further stabilize the neutral form of the probe and require more acidic condition to fully protonate the guanidino group for turn-on response. As a result, the optimal

[a]*State Key Laboratory of Bioreactor Engineering, Shanghai Frontiers Science Center of Optogenetic Techniques for Cell Metabolism, Shanghai Key Laboratory of New Drug Design, Shanghai Key Laboratory of Chemical Biology, School of Pharmacy, East China University of Science & Technology, 130 Meilong Road, Shanghai 200237, China. E-mail: xuhuan@ecust.edu.cn; kylou@ecust.edu.cn*

[b]*A Department of Pharmacology and Toxicology and BIO5 Institute, University of Arizona, Tucson, AZ 85721-0207, USA. E-mail: wwang@pharmacy.arizona.edu*

† Electronic supplementary information (ESI) available: Synthetic procedures, additional optical studies, protocols, and NMR and HRMS data. See DOI: 10.1039/d2ra00741j

‡ These two authors contribute equally to this work.

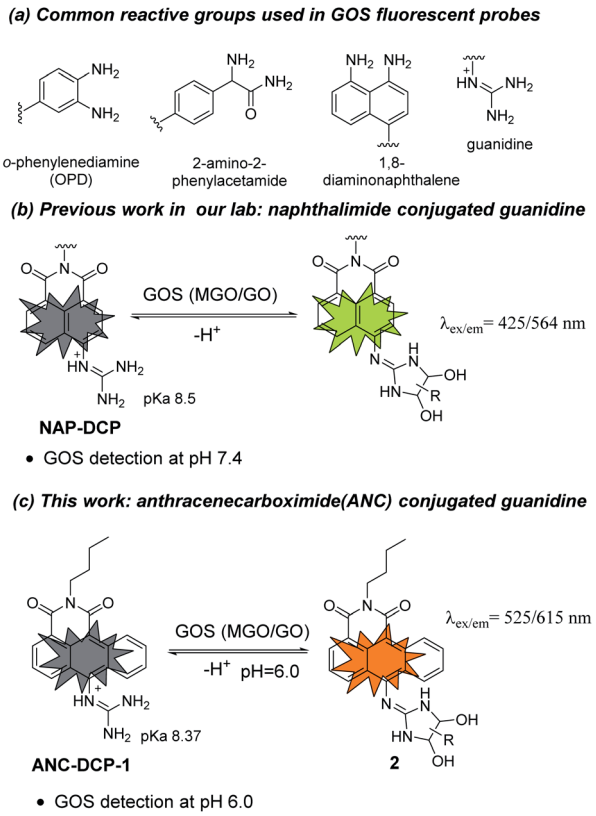

Fig. 1 Probe design: (a) common reactive groups used in GOS fluorescent probes; (b) **NAP-DCP** series of probes adopting 1,8-naphthalimide as the fluorophore; (c) this work: 1,9-anthracenedicarboxamide based fluorescent probe **ANC-DCP-1**. The extension of conjugation system lowered pK_a and pH required for full protonation of the probe.

pH of **ANC-DCP-1** for GOS detection may be lower than 7, allowing GOS detection in acidic environment.

Results and discussion

The probe **ANC-DCP-1** was conveniently synthesized from heating the corresponding anthrenecarboximide bromide **1**[31] and acetylguanidine **2** in a mixture of solvent of tetrahydrofuran and methanol in a sealed tube at 120 °C (Scheme S1†). Its structure was characterized by ^{1}H NMR, ^{13}C NMR, HRMS (see ESI† part I for more details).

With the probe in hand, we first studied the probe **ANC-DCP-1**'s UV-Vis spectra at various pHs from 12.94 to 2.78 to determine the probe's pK_a. The probe (pH ≥ 10) had an absorption peak at 496 nm, while the protonated probe (pH ≤ 6) showed an absorption peak at 443 nm (Fig. S1†). The blue-shift of the absorption peak of the protonated probe was due to the reduced intramolecular charge transfer (ICT), supported by the calculated electron density reduction at the fluorophore's 10-position from the model probe **4** to its protonated form **3** (Fig. S9†) based on DFT (TD-DFT) calculations at the B3LYP/6-31+G(d,p) level (see ESI† part III for more details).[32,33] Nonlinear fitting of the measured absorbance at 496 nm *versus* pH values afforded pK_a value of 8.37, lower than the pK_a 8.48 (ref. 29) of **NAP-DCP-1** due to the extended conjugation. UV-Vis responses of the probe for MGO and GO at three different pHs (7.4, 6.0, and 5.0) were then studied. At pH 6.0, the probe is fully protonated as expected from its pK_a value. The probe's reaction with GOS resulted in the emergence of a shoulder peak (Fig. 2a and b), presumably due to formation of the deprotonated 5-membered dihydroxyimidazolidine adducts (Fig. 1c). Selective excitation of the deprotonated adducts at 525 nm generated the fluorescence turn-on response at 615 nm (Fig. 2c). In contrast, the probe's absorption spectrum contained a shoulder peak at around 496 nm at pH 7.4 due to deprotonation (Fig. S2a and b†), which overlapped with the adducts' absorption peak and interfered with GOS detection by raising background fluorescence, while at pH 5.0, almost no changes of absorption spectra upon incubation with MGO and GO were identified (Fig. S2c and d†), suggesting low reactivity of the probe at pH 5.0. Indeed, pH-dependent fluorescence intensity studies of the probe before and after incubation with 200 equiv. MGO or GO for 2 h at 37 °C confirmed that the probe is suitable for GOS detection at weak acidic condition around pH 6.0 (Fig. S3†). Interestingly, the maximum excitation wavelength was only slightly red-shifted after the probe's reaction with GOS, while the maximum emission wavelength showed a bathochromic shift of 57 nm from 558 nm to 615 nm (Fig. S4†), indicating the GOS adducts have increased Stokes shift. From time-dependent fluorescence studies (Fig. S5†), an incubation time of 2 h was chosen for GOS detection considering both MGO and GO, which is comparable to OPD-based probes.[21–24] Fluorescence turn-on ratios for the probe incubation with 200 equiv. MGO and GO were 6.4- and 8.9-fold ($\lambda_{ex/em}$ = 525/615 nm), respectively (Fig. 2c). From

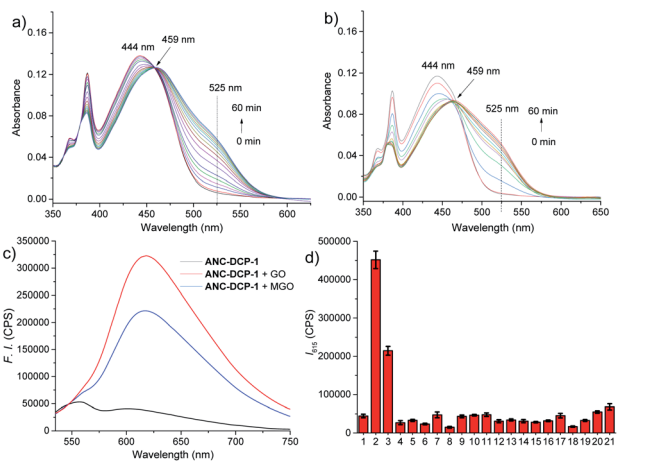

Fig. 2 (a and b) Time-dependent UV-Vis spectra of **ANC-DCP-1** (20 μM) upon addition of 200 equiv. MGO (a) or GO (b); (c) fluorescence emission spectra (λ_{ex} = 525 nm) of **ANC-DCP-1** (5 μM) before and after addition of 200 equiv. MGO or GO for 2 h; (d) fluorescence intensity of **ANC-DCP-1** (5 μM) at 615 nm (λ_{ex} = 525 nm) upon addition of various species (1 mM): (1) blank, (2) GO, (3) MGO, (4) formaldehyde, (5) benzaldehyde, (6) glyoxylic acid, (7) acetaldehyde, (8) *o*-phthalaldehyde, (9) H_2O_2, (10) glutathione, (11) cysteine, (12) homocysteine, (13) glucose, (14) Na^+, (15) Ca^{2+}, (16) Al^{3+}, (17) K^+, (18) Cu^{2+}, (19) Zn^{2+}, (20) blank (5% DMSO); (21) NOC-18 (5% DMSO).

concentration-dependent fluorescence emission studies, limits of detection (LODs) for MGO and GO were calculated as 12.6 and 12.1 μM, respectively (Fig. S6†). The probe also showed reversibility in fluorescence turn-on responses for MGO and GO (Fig. S7†), supporting similar equilibrium-based reaction mechanism as the **NAP-DCP** series of probes. Moreover, the probe retained good selectivity for GOS over many other species including formaldehyde (FA), benzaldehyde, glyoxylic acid, acetaldehyde, *o*-phthalaldehyde, H_2O_2, glutathione, cysteine, homocysteine, glucose, Na^+, Ca^{2+}, Al^{3+}, K^+, Cu^{2+}, Zn^{2+}, and NO (NOC-18) (Fig. 2d). The observed slight increase of fluorescence intensity when the probe was incubated with NOC-18 (column 21 in Fig. 2d) was mainly due to increased DMSO percentage (from 1% to 5%) in the test sample preparation as 5% DMSO induced the similar fluorescence intensity increase (column 20 in Fig. 2d). The high selectivity for GOS detection over FA was further confirmed by UV-Vis studies, as FA addition induced almost no changes in the UV-Vis spectrum (Fig. S8†).

The reaction mechanism underlying the probe **ANC-DCP-1**'s turn-on fluorescence detection for GOS and high selectivity over FA is believed to be similar to the previous studied probe **NAP-DCP-1**.[29] The guanidino group of the probe was predominately protonated at pH 6.0. After reaction with GOS, the formation of dihydroxyimidazolidine adducts, as evidenced by HRMS studies of the probe's reaction with GO and MGO (Fig. S11†), resulted in the appearance of the red-shifted shoulder peak in the UV spectra due to increased acidity and deprotonation (Fig. 2a and b). The assignment of the shoulder peak to the deprotonated adducts was supported by TD-DFT calculations on the model compounds **3**, **5**, and **6**, which could possibly exist in equilibrium at pH 6.0. The deprotonated adduct **6** give red-shifted absorption compared with both the protonated probe **3** and the protonated adduct **5** (Table S1, see ESI† part III for more details). From calculated HOMO and LUMO orbitals of the adduct **6**, significantly increased p–π conjugation between the guanidino substituent and the fluorophore was identified (Fig. S10†), which is responsible for the red-shift of the absorption. The protonated probe-GOS adducts were selectively excited at 525 nm, resulting in the observed fluorescence turn-on response. In contrast, FA cannot form cyclized adducts since the corresponding cyclization reaction requires the formation of a four-membered ring, which is both kinetically and dynamically unfavorable, providing the basis for the probe's high selectivity over FA.

We further explored the potential application of the probe **ANC-DCP-1** for GOS detection in weak acidic human urine. Fluorescence emission studies of 10 μM **ANC-DCP-1** in urine from a healthy volunteer (pH = 5.9) incubated with externally added various concentrations of MGO and GO (0 to 2 mM) showed concentration-dependent fluorescence emission increases maximized at 615 nm (Fig. S12a and b†), suggesting that the probe is capable of differentiating relative GOS levels in urine samples. The LODs of the probe for MGO and GO in urine were determined from linear regression as 7.3 and 4.7 μM (S/N), respectively (Fig. S12c and d†), which fell in the range of total GOS levels in urine of diabetic patients.[34] Since MGO and GO levels are simultaneously elevated in diabetic urine samples,[35] the GOS level in urine indicated from the fluorescence intensity increase after incubation with the probe can be potentially used for diabetes diagnosis. In a preliminary study of ten urine specimen consisting of five urine samples from five different healthy volunteers and five urine samples from distinctive diabetic patients, all diabetic urine samples showed significantly higher fluorescence intensity increases at 615 nm compared with those of the normal urine samples (Fig. 3a, b, Tables S2 and S3†), particularly for the diabetic chylous urine samples No. 3 and 4. Moreover, the fluorescence intensity increases at 615 nm in urine samples were correlated with glucose levels measured in blood by the hexokinase catalysis method (Fig. 3c, see ESI† part V for more details). The results supported the potential use of the probe for diabetic diagnosis and prognosis *via* fluorescence monitoring GOS levels in urine samples.

Finally, we investigated potential use of the probe **ANC-DCP-1** for studying MGO levels in Manuka honey, which is known for its non-peroxide antibacterial activity (NPA) attributing mainly to its high MGO levels (up to 700–800 mg kg^{-1}).[36] Traditionally, MGO levels in Manuka honey are measured by HPLC methods, which often require lengthy sample derivatization.[36,37] Considering very low level of GO compared with much higher MGO levels presented in Manuka honey,[36] the probe's turn-on fluorescence at 615 nm can provide an attractive way for fast evaluation of MGO levels in Manuka honey. For convenience, Acacia honey was selected as the low MGO control honey to imitate the de-MGO Manuka honey. To confirm the low MGO content of the Acacia honey, a mixture of 1 g of acacia honey and 9 g of pH 6.5

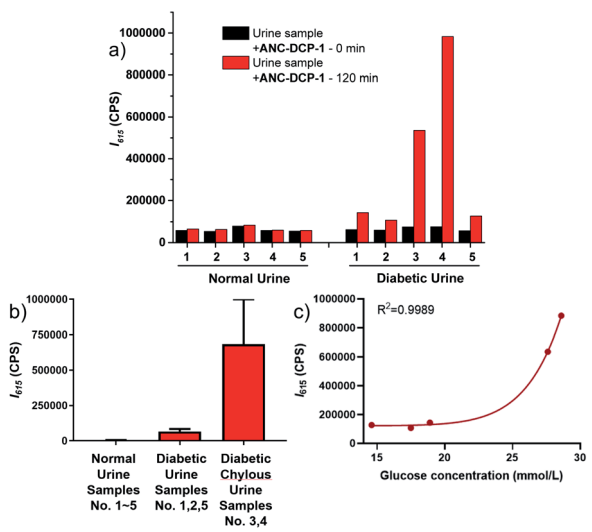

Fig. 3 (a) Fluorescence intensities of different urine samples at 615 nm (λ_{ex} = 525 nm) observed immediately (black columns) after addition of ANC-DCP-1 (10 μM) *versus* observed after 2 h incubation at 37 °C and pH 6.0 (red columns); (b) comparison of fluorescence intensity increases at 615 nm (λ_{ex} = 525 nm) after 2 h incubation at 37 °C and pH 6.0 for normal urine samples, diabetic urine samples not being chylous, and diabetic urine samples being chylous; (c) nonlinear regression of the measured fluorescence intensity increases at 615 nm (λ_{ex} = 525 nm) in the urine specimen and the corresponding blood glucose concentrations (mmol L^{-1}) of the five diabetic patients.

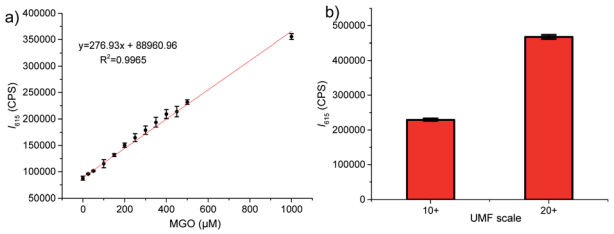

Fig. 4 (a) Linear regression of fluorescence intensity at 615 nm (λ_{ex} = 525 nm) of the probe **ANC-DCP-1** (10 μM) in diluted acacia honey (pH 6.0) incubated at 37 °C for 1 h *versus* the concentrations (0–1000 μM) of MGO added; (b) measured fluorescence intensity at 615 nm (λ_{ex} = 525 nm) of the probe **ANC-DCP-1** (10 μM) in the two diluted Manuka honey samples (pH 6.0) incubated at 37 °C for 1 h.

PBS solution with a final pH 6.0 was incubated with 10 μM probe at 37 °C for 1 h, and very low fluorescence intensity increase was identified (Fig. S13a†). Addition of various concentrations (0 to 1 mM) of MGO to the above diluted acacia honey solution (pH 6.0) containing 10 μM probe induced concentration-dependent fluorescence emission increases (Fig. S13b†) with good linear relationship at 615 nm (Fig. 4a, R^2 = 0.997). We then tested two purchased Manuka honey samples labelled with unique Manuka factor (UMF) values 10+ ([MGO] > 256 mg kg^{-1}) and 20+ ([MGO] > 829 mg kg^{-1}). The similarly prepared diluted Manuka honey samples (pH 6.0) were incubated with 10 μM probe at 37 °C for 1 h. Fluorescence intensities at 615 nm (λ_{ex} = 525 nm) were measured (Fig. 4b). Using the standard curve obtained from acacia honey (Fig. 4a), the deduced MGO levels from the fluorescence intensities at 615 nm were 366 ± 8 and 984 ± 16 mg kg^{-1}, respectively, which matched well with their labelled UMF scales. The results suggested that the probe has great potentials for fast UMF scale determination of Manuka honey.

Conclusions

In conclusion, we reported an anthracenecarboximide-guanidine based fluorescent probe **ANC-DCP-1** for selective turn-on detection of methylglyoxal and glyoxal (GOS) over formaldehyde. Compared with the previously reported 1,8-naphathalimide-guanidine based fluorescent probes, replacement of the naphthalene ring with an anthracene ring lowers the probe's pK_a, enabling the probe's turn-on detection of GOS at weak acidic condition around pH 6.0. The probe showed great potentials in studying relative GOS levels in weak acidic biological fluids such as in urine for diabetic diagnosis and prognosis, and also found applications in food industries such as for fast UMF scale determination of Manuka honey.

Author contributions

Junwei Chen: investigation, writing-original draft, formal analysis. Yuna Lin: investigation, formal analysis. Wanjin Xing: validation. Xingchen Zhang: validation. Huan Xu: methodology, resources, funding acquisition, writing-review & editing. Wei Wang: supervision, Writing-review & editing. Kaiyan Lou: conceptualization, project administration, funding acquisition, writing-review & editing.

Conflicts of interest

The authors declare no competing interests.

Acknowledgements

This work was supported by Shanghai Natural Science Fund (Grant No. 20ZR1414700), Shanghai Frontiers Science Centre of Optogenetic Techniques for Cell Metabolism (Shanghai Municipal Education Commission), Shanghai Sailing Program (Grant No. 19YF1412500), the National Natural Science Foundation of China (Grant No. 21577037, 21738002, 21906057, 42177417), the State Key Laboratory of Bioreactor Engineering.

Notes and references

1 M. P. Kalapos, *Toxicol. Lett.*, 1999, **110**, 145–175.
2 N. Rabbani and P. J. Thornalley, *Amino Acids*, 2012, **42**, 1133–1142.
3 N. Shangari, W. R. Bruce, R. Poon and P. J. O'Brien, *Biochem. Soc. Trans.*, 2003, **31**, 1390–1393.
4 P. J. Thornalley, *Ann. N. Y. Acad. Sci.*, 2005, **1043**, 111–117.
5 G. Vistoli, D. De Maddis, A. Cipak, N. Zarkovic, M. Carini and G. Aldini, *Free Radical Res.*, 2013, **47**, 3–27.
6 S. A. Phillips and P. J. Thornalley, *Eur. J. Biochem.*, 1993, **212**, 101–105.
7 G. A. Lyles and J. Chalmers, *Biochem. Pharmacol.*, 1992, **43**, 1409–1414.
8 Z. S. Agadjanyan, S. F. Dugin and L. F. Dmitriev, *Mol. Cell. Biochem.*, 2006, **289**, 49–53.
9 P. J. Thornalley, A. Langborg and H. S. Minhas, *Biochem. J.*, 1999, **344**, 109–116.
10 A. Mlakar, A. Batna, A. Dudda and G. Spiteller, *Free Radic. Res.*, 1996, **25**, 525–539.
11 B. Mannervik, *Drug Metab. Drug Interact.*, 2008, **23**, 13–27.
12 S.-Y. Goh and M. E. Cooper, *J. Clin. Endocrinol. Metab.*, 2008, **93**, 1143–1152.
13 A. Prasad, P. Bekker and S. Tsimikas, *Cardiol. Rev.*, 2012, **20**, 177–183.
14 A. K. Berner, O. Brouwers, R. Pringle, I. Klaassen, L. Colhoun, C. McVicar, S. Brockbank, J. W. Curry, T. Miyata, M. Brownlee, R. O. Schlingemann, C. Schalkwijk and A. W. Stitt, *Diabetologia*, 2012, **55**, 845–854.
15 J. Masania, M. Malczewska-Malec, U. Razny, J. Goralska, A. Zdzienicka, B. Kiec-Wilk, A. Gruca, J. Stancel-Mozwillo, A. Dembinska-Kiec, N. Rabbani and P. J. Thornalley, *Glycoconjugate J.*, 2016, **33**, 581–589.
16 D. Schroeter and A. Hoehn, *Curr. Pharm. Design*, 2018, **24**, 5245–5251.
17 C. Angeloni, L. Zambonin and S. Hrelia, *Biomed. Res. Int.*, 2014, 238485.
18 N. Shangari and P. J. O'Brien, *Biochem. Pharmacol.*, 2004, **68**, 1433–1442.

19 J. Degen, M. Hellwig and T. Henle, *J. Agric. Food Chem.*, 2012, **60**, 7071–7079.
20 L. R. Bhat, S. Vedantham, U. M. Krishnan and J. B. B. Rayappan, *Biosens. Bioelectron.*, 2019, **133**, 107–124.
21 T. Wang, E. F. Douglass Jr, K. J. Fitzgerald and D. A. Spiegel, *J. Am. Chem. Soc.*, 2013, **135**, 12429–12433.
22 M. Yang, J. Fan, J. Zhang, J. Du and X. Peng, *Chem. Sci.*, 2018, **9**, 6758–6764.
23 S. Gao, Y. Tang and W. Lin, *J. Fluoresc.*, 2019, **29**, 155–163.
24 Y. Dang, F. Wang, L. Li, Y. Lai, Z. Xu, Z. Xiong, A. Zhang, Y. Tian, C. Ding and W. Zhang, *Chem. Commun.*, 2020, **56**, 707–710.
25 H. Wang, Y. Xu, L. Rao, C. Yang, H. Yuan, T. Gao, X. Chen, H. Sun, M. Xian, C. Liu and C. Liu, *Anal. Chem.*, 2019, **91**, 5646–5653.
26 A. Jana, M. Baruah, S. Munan and A. Samanta, *Chem. Commun.*, 2021, **57**, 6380–6383.
27 Y. Tang, Y. Ma, J. Yin and W. Lin, *Chem. Soc. Rev.*, 2019, **48**, 4036–4048.
28 G. Burgos-Barragan, N. Wit, J. Meiser, F. A. Dingler, M. Pietzke, L. Mulderrig, L. B. Pontel, I. V. Rosado, T. F. Brewer, R. L. Cordell, P. S. Monks, C. J. Chang, A. Vazquez and K. J. Patel, *Nature*, 2017, **548**, 549–554.
29 H. Xu, Q. Liu, X. Song, C. Wang, X. Wang, S. Ma, X. Wang, Y. Feng, X. Meng, X. Liu, W. Wang and K. Lou, *Anal. Chem.*, 2020, **92**, 13829–13838.
30 B.-B. Lind, Z. Ban and S. Bydén, *Bioresour. Technol.*, 2000, **73**, 169–174.
31 Z. Gao, B. Han, K. Chen, J. Sun and X. Hou, *Chem. Commun.*, 2017, **53**, 6231–6234.
32 H. Tong, Y. Zheng, L. Zhou, X. Li, R. Qian, R. Wang, J. Zhao, K. Lou and W. Wang, *Anal. Chem.*, 2016, **88**, 10816–10820.
33 M. J. Frisch, G. W. Trucks, H. B. Schlegel, G. E. Scuseria, M. A. Robb, J. R. Cheeseman, G. Scalmani, V. Barone, B. Mennucci, G. A. Petersson, H. Nakatsuji, M. Caricato, X. Li, H. P. Hratchian, A. F. Izmaylov, J. Bloino, G. Zheng, J. L. Sonnenberg, M. Hada, M. Ehara, K. Toyota, R. Fukuda, J. Hasegawa, M. Ishida, T. Nakajima, Y. Honda, O. Kitao, H. Nakai, T. Vreven, J. A. Montgomery Jr, J. E. Peralta, F. Ogliaro, M. J. Bearpark, J. Heyd, E. N. Brothers, K. N. Kudin, V. N. Staroverov, R. Kobayashi, J. Normand, K. Raghavachari, A. P. Rendell, J. C. Burant, S. S. Iyengar, J. Tomasi, M. Cossi, N. Rega, N. J. Millam, M. Klene, J. E. Knox, J. B. Cross, V. Bakken, C. Adamo, J. Jaramillo, R. Gomperts, R. E. Stratmann, O. Yazyev, A. J. Austin, R. Cammi, C. Pomelli, J. W. Ochterski, R. L. Martin, K. Morokuma, V. G. Zakrzewski, G. A. Voth, P. Salvador, J. J. Dannenberg, S. Dapprich, A. D. Daniels, Ö. Farkas, J. B. Foresman, J. V. Ortiz, J. Cioslowski and D. J. Fox, *Gaussian 09*, Gaussian, Inc., Wallingford, CT, USA, 2009.
34 L. A. Zardari, M. Y. Khuhawar and A. J. Laghari, *Chromatographia*, 2009, **70**, 891–897.
35 K. Akira, Y. Matsumoto and T. Hashimoto, *Clin. Chem. Lab. Med.*, 2004, **42**, 147–153.
36 E. Mavric, S. Wittmann, G. Barth and T. Henle, *Mol. Nutr. Food Res.*, 2008, **52**, 483–489.
37 C. J. Adams, C. H. Boult, B. J. Deadman, J. M. Farr, M. N. C. Grainger, M. Manley-Harris and M. J. Snow, *Carbohydr. Res.*, 2008, **343**, 651–659.